GEOPHYSICAL RESEARCH LETTERS, VOL. 36, L15803, doi:10.1029/2009GL038727, 2009

Ice particle growth in the polar summer mesosphere: Formation time and equilibrium size

A. Y. Zasetsky,[1] S. V. Petelina,[2] R. Remorov,[3] C. D. Boone,[3] P. F. Bernath,[4,5] and E. J. Llewellyn[6]

Received 15 April 2009; revised 9 June 2009; accepted 1 July 2009; published 1 August 2009.

[1] The growth kinetics for ice particles in the polar summer mesosphere is studied using the density of water vapor, temperature, and total ice volume simultaneously measured by the infrared Fourier Transform Spectrometer on the Atmospheric Chemistry Experiment (ACE-FTS) satellite. The results are based solely on the ACE-FTS retrievals, without using any adjustable parameters. The computed particle formation time is in the range between 2 hours at 150 K and 20 hours at 120 K, during which particles come to equilibrium with water vapor and reach the size of 20–70 nm. The growth rate varies from 0.2 nm/hour to 30 nm/hour in the temperature range analyzed. As it takes ice crystals only 20 minutes to grow by 10 nm at 150 K, the transition from optically subvisible to the visible size range can occur on a time scale of minutes. This could account for fast variations in PMC brightness observed recently. **Citation:** Zasetsky, A. Y., S. V. Petelina, R. Remorov, C. D. Boone, P. F. Bernath, and E. J. Llewellyn (2009), Ice particle growth in the polar summer mesosphere: Formation time and equilibrium size, *Geophys. Res. Lett.*, *36*, L15803, doi:10.1029/2009GL038727.

1. Introduction

[2] Understanding the process of ice particle formation in Polar Mesospheric Clouds (PMCs), including the nucleation rate and growth kinetics, is important as PMCs provide valuable information on physical and dynamical processes in the upper mesosphere. Knowledge of these processes is also vital for the correct interpretation of the observed variability and trends in cloud properties [*Shettle et al.*, 2009; *Petelina et al.*, 2007]. As PMC properties are governed primarily by the water vapor pressure and temperature, it has been suggested that the observed long-term trends in the frequency of PMC occurrence and their brightness may serve as a sensitive indicator of changes in climate [e.g., *Thomas*, 2003].

[3] In comparison to a decade ago, much more is now known about the upper mesospheric environment in general and PMCs in particular. This is largely due to a significant increase in the number and sophistication of satellite-borne and ground-based instruments [e.g., *Rapp and Lübken*, 2004; *DeLand et al.*, 2006; *Russell et al.*, 2009]. However, the mechanism of mesospheric ice nucleation, the ice particle number density and size distribution as well as the rate at which new ice particles form are still poorly known. In the present work we study the kinetics of mesospheric ice growth by solving the differential equations that describe the balance between condensation and desorption fluxes of water vapor on ice particles. The growth rates are computed using the total volume of ice in the mesosphere, temperature, and water vapor density measured by the Fourier Transform Spectrometer on the Atmospheric Chemistry Experiment (ACE-FTS) satellite. The use of parameters observed simultaneously by a single instrument is undoubtedly advantageous over the studies performed with more than one satellite and/or ground-based instruments [e.g., *Petelina et al.*, 2005].

2. Instrument and Data Description

2.1. ACE-FTS Instrument

[4] ACE was launched in 2003 in a circular orbit at 650 km altitude with an inclination of 74° and latitudinal coverage from 85°N to 85°S [*Bernath et al.*, 2005]. The FTS is the primary instrument on ACE, and has a spectral resolution of 0.02 cm^{-1} with spectral coverage from 750 to 4400 cm^{-1}. The ACE-FTS measures the atmospheric transmittance in occultation mode during sunrise and sunset. The instrument field of view (FOV) is 1.25 mrad, which corresponds to about 4 km at the tangent point. The latitudinal coverage changes throughout the year [*Bernath*, 2006] and the highest latitudes for ACE-FTS measurements used in this work do not extend poleward of 70°.

2.2. ACE-FTS Pressure, Temperature, and Water Vapor Density

[5] The retrieval method for temperature, and water vapor volume mixing ratio (VMR) is described in detail by *Boone et al.* [2005]. About 60 microwindows in the 950–975 cm^{-1} and 1360–2000 cm^{-1} regions are used to retrieve H_2O profiles between 5 and 90 km. Because of the high spectral resolution of 0.02 cm^{-1}, no special corrections are needed in the presence of PMCs. Isolated CO_2 lines are used to derive the values of pressure and temperature. In the mesosphere these CO_2 lines are in the 2050–2070 cm^{-1} and 2300–2390 cm^{-1} ranges, where the spectral contribution from PMC particles to the baseline is very weak.

[1]Kurnakov Institute of General and Inorganic Chemistry, Russian Academy of Sciences, Moscow, Russia.
[2]Department of Physics, La Trobe University, Melbourne, Victoria, Australia.
[3]Waterloo Center for Atmospheric Sciences, University of Waterloo, Waterloo, Ontario, Canada.
[4]Also at Waterloo Center for Atmospheric Sciences, University of Waterloo, Waterloo, Ontario, Canada.
[5]Department of Chemistry, University of York, Heslington, UK.
[6]Institute of Space and Atmospheric Science, University of Saskatchewan, Saskatoon, Saskatchewan, Canada.

0094-8276/09/2009GL038727$05.00

Therefore, the effect of the presence of ice particles on the retrieved VMRs and temperature is negligible and uncertainties in the retrieved pressure and temperature are given by the statistical fitting errors.

[6] Comparison of ACE temperatures with several coincident measurements gives an agreement of better than 5 K for the lower mesosphere and better than 8 K for the upper mesosphere [*Sica et al.*, 2008]. There is some evidence for a systematic high bias of 3–6 K at 50–70 km, but no indication of any bias at the PMC altitudes. The random uncertainty of 8 K in the upper mesosphere can, in part, result from the altitude resolution of 4 km for the ACE-FTS, which is often too low to capture details on structures such as mesospheric inversion layers. The deviations are also of geophysical origin, a result of spatial and temporal separations between coincident observations made by different instruments.

[7] The ACE-FTS water VMR retrievals were validated by *Carleer et al.* [2008], where the uncertainty was reported to be better than 5–10% from 15 to 70 km and about 8% below 83 km. The results of *Lambert et al.* [2007] give a relative difference between the Microwave Limb Souder (MLS) on Aura and ACE-FTS H_2O profiles of less than 5% at the altitudes below 0.01 hPa. Although these results indicate the good accuracy of the ACE-FTS mixing ratio retrievals in the upper mesosphere, there is an inherent averaging that arises from the viewing geometry and high variability of gaseous water in the presence of PMCs due to the patchy structure of clouds and large temperature gradients along the optical path of about 500 km. From a statistical viewpoint, as a very long path is sampled, although the mean of a retrieved value may not be affected, the dispersion (or error) for water VMR retrievals can be relatively high. The precise estimate of this error, however, requires the use of atmospheric models, which is beyond the scope of the present study.

2.3. PMC Detection and Ice Volume

[8] PMCs are detected by the ACE-FTS in three distinct spectral regions, namely: the librational mode centered at 800 cm^{-1}, bending mode at 1600 cm^{-1}, and O-H stretching mode between 3000 and 3500 cm^{-1} [*Eremenko et al.*, 2005]. The ice signal is most intense in the O-H stretching band, and the infrared absorption intensity is proportional to the total ice volume along the line-of-sight. In this work, we analyze more than 300 PMC events observed in the northern hemisphere during 5–20 July of 2005 at latitudes 60°–70°N. In order to ensure a good quality of results, only those PMC observations are considered in which the ratio of peak ice absorption signal to baseline noise in the O-H stretching band is 5 or higher.

[9] In order to determine the total amount of water in the upper mesosphere and calculate the formation time for PMC particles, the volume of ice per cubic centimeter of atmosphere is required. For this, and to account for the patchy structure of PMCs, the cloud optical path length has to be assumed. Here, it is arbitrarily taken to be half of the total path length for mesospheric ACE-FTS observations, which is about 250 km. This uncertainty dominates the error budget as it significantly exceeds all other uncertainties, such as fitting errors, inaccuracies in the optical constants, etc. Our estimate for the total uncertainty in the calculated ice volume is thus ±50%.

[10] For illustration and comparison purposes we discuss the PMC density in terms of the ice number density, n_{Ice}. Since the ACE-FTS spectra are not sensitive to the variations in sizes from 10 to 100 nm (and are insensitive to particles with radii smaller than 10 nm), some effective value for the particle radius needs to be assigned. In this work, we use randomly oriented hexagonal prisms with an equivalent-volume-radius of 60 nm. This radius value was retrieved from the (nearly) coincident PMC observations of the Optical Spectrograph and InfraRed Imager System (OSIRIS) on Odin made in the same latitude region in 5–20 July 2005 [*Eremenko et al.*, 2005]. We stress that the choice of effective radius value does not affect in any way the results of our calculations. Note also that the use of an effective size of 30 nm instead of 60 nm would increase the number density of ice particles by an order of magnitude.

[11] For PMCs registered by ACE-FTS, the retrieved n_{Ice} values are between 20 cm^{-3} and 130 cm^{-3}. We note that while the highest n_{Ice} value is 130 cm^{-3}, the probability of finding a cloud with a density higher than 50 cm^{-3} is rather low. These values for n_{Ice} are in good agreement with the results of 10 years of ground-based lidar measurements at 69°N and 16°E reported by *Baumgarten et al.* [2008], where typical n_{Ice} values are reported to be in the range between 33 and 105 cm^{-3}. At the same time, recent results from the Solar Occultation For Ice Experiment (SOFIE) on the Aeronomy of Ice in the Mesosphere (AIM) satellite give different values for n_{Ice}, between 200 and 300 cm^{-3} in 5–20 July of 2007 [*Hervig et al.*, 2009]. This disagreement may be explained by somewhat different geographic locations of SOFIE observations (70–72°N) and its sensitivity to smaller ice particles with radii of 5–10 nm.

3. Mesospheric Ice Growth Time and Equilibrium Size

[12] In this section, the rate of mesospheric ice growth is calculated using the total water (in solid and gas phase) and temperature measured by the ACE-FTS. It is assumed that for a given atmospheric state, time is the only factor affecting the abundance and size of ice particles, the temperature of the PMCs does not vary, and the ice particles are only growing, but not sublimating.

[13] For mesospheric conditions, the condensation of water vapor on the surface of mesospheric aerosols occurs based on the Knudsen number K_n, i.e., when $K_n \gg 1$. In this case, the growth of ice crystals is described by a well-known equation for the difference between the condensation and desorption fluxes of water vapor molecules through the interface:

$$\frac{dr}{dt} = \frac{m_{H2O}}{\rho_{Ice}}\left(k_a n_g - k_d n_s\right). \quad (1)$$

In equation (1), r is the particle radius, m_{H2O} is the mass of the water molecule, ρ_{Ice} is the density of ice, k_a is the adsorption rate, n_g is the H_2O concentration (density) in the gas phase, k_d is the desorption rate, n_s is the surface concentration of H_2O. The first and second terms on the right side of equation (1) are the adsorption and desorption fluxes, respectively. The adsorption rate constant is defined as $k_a = \alpha c/4$, where α is the probability of adsorption

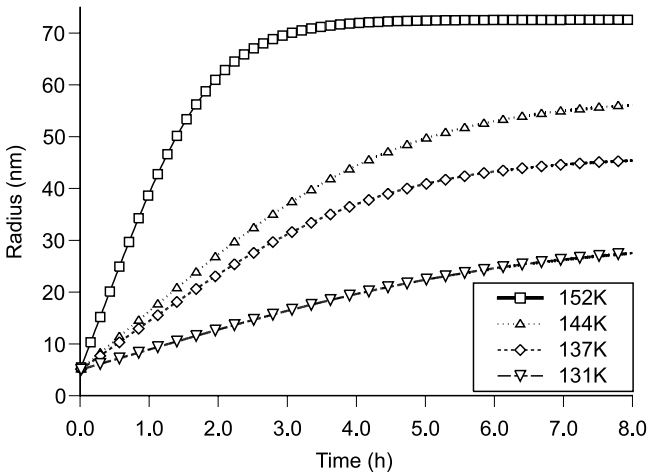

Figure 1. Kinetics of mesospheric ice particle growth calculated using the ACE-FTS PMC observations.

(sticking probability coefficient) and c is the thermal speed. The desorption flux can be found from specific balance

$$k_d n_s = k_a n_{eq}, \tag{2}$$

where n_{eq} is the density of water vapor over ice corrected by the Kelvin relation for the curvature effect on the surface tension of ice γ_∞, which takes into account the increase in the internal pressure of ice particles with decreasing radius. Expressing n_{eq} in terms of γ_∞ gives

$$k_d n_s = k_a n^o_{eq} \exp\left(\frac{2\gamma_\infty m_{H2O}}{RT\rho_{Ice} r}\right), \tag{3}$$

where n^o_{eq} is the equilibrium density of water vapor over a flat surface.

[14] The uptake of water molecules by ice particles is defined by adsorption and desorption:

$$\frac{dn_g}{dt} = \left(-k_a n_g + k_a n^o_{eq} \exp\left(\frac{2\gamma_\infty m_{H2O}}{RT\rho_{Ice} r}\right)\right) 4\pi r^2 n_{Ice}, \tag{4}$$

After some algebra, equations (1) and (4) can be rewritten as

$$\frac{dr}{dt} = \frac{m_{H2O}}{4\rho_{Ice}} c n^o_{eq} \left[\alpha S - \exp\left(\frac{2\gamma_\infty m_{H2O}}{RT\rho_{Ice} r}\right)\right] \tag{5}$$

$$\frac{dn_g}{dt} = \left[-\alpha S + \exp\left(\frac{2\gamma_\infty m_{H2O}}{RT\rho_{Ice} r}\right)\right] \pi r^2 c n^o_{eq} n_{Ice} \tag{6}$$

where S is the vapor saturation ratio.

[15] By solving the differential equations (5) and (6) numerically, we can determine the saturation values for ice particle equilibrium size. To approximate the conditions when the PMCs were formed, we assign the amount of water observed in the ice phase to the gaseous state. The calculations are then initialized using total water as the sum of observed gas and ice phase water abundance. The ratio of virtual vapor pressure to the equilibrium pressure is then computed using the Murphy-Koop relation [*Murphy and Koop*, 2005]. Parameters used in these calculations that were retrieved from ACE-FTS are: S from 1.5 to 2.0; water vapor density from $4 \cdot 10^8$ to $3 \cdot 10^9$ cm^{-3}; temperature from 120 to 165 K; ice volume between $2.26 \cdot 10^7$ and $1.18 \cdot 10^8$ μm^3/cm^3. The surface tension is 0.0122 H/m [*Hale and Plummer*, 1974] and ρ_{Ice} = 0.93 g/cm^3. The only adjustable parameter in the kinetic model is the sticking probability coefficient α that is taken to be 1 in the present work. Experimental and theoretical studies suggest the range for α for different temperatures and pressures is between 0.8 and 1 with unity being the most probable value for typical thermodynamic conditions in the upper mesosphere [*Batista et al.*, 2005, and references therein].

[16] In view of the extremely high sensitivity of the growth rate to temperature, the uncertainty of 8 K in the ACE-FTS temperature may result in significant, up to 200%, errors in the calculated particle growth time. This uncertainty, however, is random and thus will be reduced by averaging over many observations.

4. Results and Discussion

[17] The calculated growth curves for ice particles for four representative PMC observations with the same saturation S (occultation numbers: ss10206, T = 152 K; ss10283, T = 144 K; ss10289, T = 137 K; ss10358, T = 131 K) are shown in Figure 1. It is seen that the particle growth time increases with decreasing temperature and corresponding reduction in the density of water vapor. The growth curves feature two regions: (a) the initial regime of fast growth (from which we determine the growth rate *dr*/*dt*) and the flat region where the excess (supersaturation) of water vapor is exhausted and the final vapor-ice equilibrium is reached. Note that in order to better illustrate the fast growth regime, the flat regions in Figure 1 are not shown for all temperatures, but just for 152 K. Once equilibrium is reached we obtain the equilibrium size for PMC particles, which corresponds to the flat region in the growth curve. The analysis of more than 300 ACE-FTS cloud observations made in 5–20 July, 2005 gives the equilibrium particle radius to be in the range between 20 and 70 nm. The equilibrium size strongly depends on the water vapor density and temperature. The values for equilibrium radius reported in this work do not contradict the current knowledge of PMC microphysics. The most recent data on PMC particle sizes from SOFIE/AIM observations in the northern hemisphere in 2007 [*Hervig et al.*, 2009] give, in general, radii between 20 and 70 nm (with the sizes larger than 70 nm and smaller than 20 nm also being sometimes observed).

[18] The ice formation time computed as a function of temperature for ACE-FTS PMCs observations is shown in Figure 2. For all cloud events considered in this work the particle formation time varies from less than 2 hours at 150 K to 22 hours at 120 K. As noted earlier, due to the horizontal smoothing and 4 km vertical FOV of ACE-FTS, it is possible that some values of temperatures in Figure 2 may not be the true temperatures in PMCs. Higher temperatures could be reported when the instrument observes a PMC in the upper part of its FOV, while the lower part of the FOV looks at the atmosphere at 79–81 km. As the temperature lapse rate in the upper mesosphere is high, 5–8 K per km [*Lübken*, 1999], it may result in a 10–20 K increase in temperature for a PMC-containing scan. Some data points in Figure 2 that show PMCs at temperatures between 150 and 170 K, up to 20 K higher than the typical frost point temperature at these

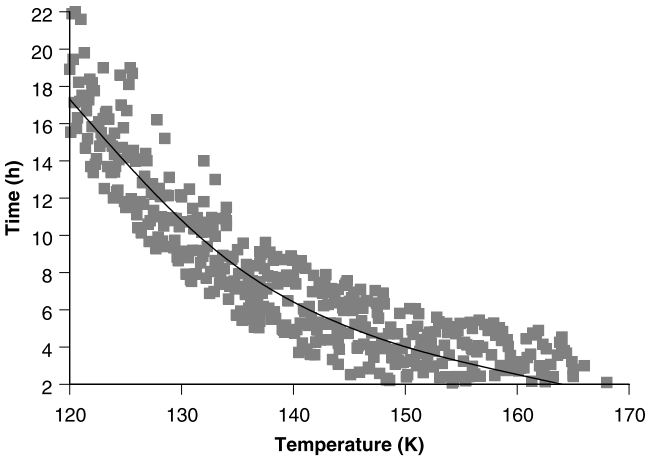

Figure 2. PMC formation time versus temperature required for ice particles to reach the equilibrium size.

altitudes, can be attributed to the effect described above. Similarly, larger water VMR (density) values can be observed when the region near 79–81 km – a high water vapor concentration due to ice particle evaporation – is observed together with a PMC located in the upper part of the FOV. The random uncertainty in temperature, which can reach 8 K, may result in 200% error in the particle growth time. However, since more than 300 ACE-FTS observations are used, the results and conclusions of this work should not be significantly altered by these uncertainties.

[19] According to our results illustrated in Figure 1, mesospheric ice particles can reach equilibrium size in a time interval of 2 hours at 150 K and of nearly 1 day at 120 K. In addition, an increase in radius by 10 nm may take only 20 minutes at 150 K. This is different from other studies of mesospheric ice growth. Results of *von Zahn and Berger* [2003] suggest that optically visible ice particles with a radius of about 30 nm grow from sub-visible particles with initial radius of 15 nm in nearly 12 hours. A model of *Mauersberger and Krankowsky* [2003] predicts the growth and sedimentation lifetime for PMC ice particles on the order of 1 day. The results from the CARMA microphysical model suggest a time of 1 to 2 days for ice particles to reach maturity and become optically visible [*Rapp and Thomas*, 2006]. *Hoffmann et al.* [2005] conclude that the formation of PMC particles with a radius of 50 nm takes about 7 hours. The analysis of ground-based lidar and radar measurements by *Gerding et al.* [2007] indicates that the particle formation time is likely more than 1 hour.

[20] Our results can assist in explaining the rapid variability in PMC brightness observed from the ground and also the recent Cloud Imaging and Particle Size Experiment (CIPS) on AIM data, where the cloud brightness shows significant variations from orbit to orbit that are 96 minutes apart [*Rusch et al.*, 2009]. As the PMC brightness observed from the ground and by AIM depends strongly on the particle size, a small increase in size would result in a large increase in brightness. According to our calculations, a 10–20 nm increase in radius can occur in 20–40 minutes at temperatures around 150 K, a region near the cloud bottom where larger particles are typically observed [e.g., *von Savigny et al.*, 2005]. As *Hervig et al.* [2009] suggest that very small ice particles are present in the upper mesosphere most of the time during the PMC season, a 10–20 nm increase in particle radii that causes notable and fast variations in PMC brightness may be possible.

5. Summary

[21] The equilibrium size and growth kinetics of ice particles in the polar summer mesosphere are computed using ACE-FTS data on the water vapor density, ice volume, and temperature measured between 5–20 July, 2005. The analysis of more than 300 cloud observations gives the ice growth rate, dr/dt, in the range from 0.2 nm/hour at 120 K to 30 nm/hour at 150 K. As expected, the growth rate is governed primarily by temperature. The particle formation time, which is the time required to reach equilibrium with water vapor, varies from 22 hours at 120 K to 2 hours at 150 K. The computed values for the ice growth rate are somewhat higher than previously assumed, with the majority of earlier studies suggesting that the PMC particle growth to optically visible sizes takes from several hours to about one day.

[22] Using the total water retrieved from the ACE-FTS spectra as an input parameter, the equilibrium particle radius is determined in the range of 20 to 70 nm. While this finding does not contradict the results of other recent studies, it is very likely that most PMC particles are not in equilibrium. Due to high temporal and spatial variability of thermodynamic conditions in the mesosphere, temperature in particular, remote sensing instruments probably take a snapshot of either growing or shrinking ice particles that are not close to equilibrium with gaseous water.

[23] In contrast to previous studies, our calculations suggest a relatively fast growth of ice particles from the optically subvisible to optically visible size range. Only 20 minutes are required for the particles to grow by 10 nm at a temperature of 150 K. This could account for recently reported remote sensing observations of PMCs, where large variations in PMC brightness are found to occur on a time scale of minutes.

[24] **Acknowledgments.** The authors are grateful to Gary Thomas (University of Colorado, USA) for useful discussions. In part this work was supported by the Natural Sciences and Engineering Research Council of Canada and the Canadian Space Agency. The Atmospheric Chemistry Experiment (ACE), also known as SCISAT, is a Canadian-led mission mainly supported by the Canadian Space Agency (CSA). Some support was also provided by the UK Natural Environment Research Council (NERC).

References

Batista, E. R., et al. (2005), What determines the sticking probability of water molecules on ice?, *Phys. Rev. Lett.*, *95*, 223201, doi:10.1103/PhysRevLett.95.223201.

Baumgarten, G. K., J. Fiedler, F.-J. Lübken, and G. von Cossart (2008), Particle properties and water content of noctilucent clouds and their interannual variations, *J. Geophys. Res.*, *113*, D06203, doi:10.1029/2007JD008884.

Bernath, P. F. (2006), Atmospheric Chemistry Experiment (ACE): Analytical chemistry from orbit, *Trends Anal. Chem.*, *25*, 647–654, doi:10.1016/j.trac.2006.05.001.

Bernath, P. F., et al. (2005), Atmospheric Chemistry Experiment (ACE): Mission overview, *Geophys. Res. Lett.*, *32*, L15S01, doi:10.1029/2005GL022386.

Boone, C. D., et al. (2005), Retrievals for the Atmospheric Chemistry Experiment Fourier-transform spectrometer, *Appl. Opt.*, *44*, 7218–7231, 8445, doi:10.1364/AO.44.007218.

Carleer, M. R., et al. (2008), Validation of water vapour profiles from the Atmospheric Chemistry Experiment (ACE), *Atmos. Chem. Phys. Discuss.*, *8*, 4499–4559.

DeLand, M. T., et al. (2006), A quarter-century of satellite polar mesospheric cloud observations, *J. Atmos. Sol. Terr. Phys.*, *68*, 9–29, doi:10.1016/j.jastp.2005.08.003.

Eremenko, M. N., S. V. Petelina, A. Y. Zasetsky, B. Karlsson, C. P. Rinsland, E. J. Llewellyn, and J. J. Sloan (2005), Shape and composition of PMC particles derived from satellite remote sensing measurements, *Geophys. Res. Lett.*, *32*, L16S06, doi:10.1029/2005GL023013.

Gerding, M., J. Höffner, M. Rauthe, W. Singer, M. Zecha, and F.-J. Lübken (2007), Simultaneous observation of noctilucent clouds, mesospheric summer echoes, and temperature at a midlatitude station (54°N), *J. Geophys. Res.*, *112*, D12111, doi:10.1029/2006JD008135.

Hale, B. N., and P. L. M. Plummer (1974), Molecular model for ice clusters in a supersaturated vapor, *J. Chem. Phys.*, *61*, 4012–4019, doi:10.1063/1.1681694.

Hervig, M. E., et al. (2009), SOFIE PMC observations during the northern summer of 2007, *J. Atmos. Sol. Terr. Phys.*, *71*, 331–339, doi:10.1016/j.jastp.2008.08.010.

Hoffmann, P., M. Rapp, A. Serafimovich, and R. Latteck (2005), On the occurrence and formation of multiple layers of polar mesosphere summer echoes, *Geophys. Res. Lett.*, *32*, L05812, doi:10.1029/2004GL021409.

Lambert, A., et al. (2007), Validation of the Aura Microwave Limb Sounder stratospheric water vapour and nitrous oxide measurements, *J. Geophys. Res.*, *112*, D24S36, doi:10.1029/2007JD008724.

Lübken, F.-J. (1999), Thermal structure of the Arctic summer mesosphere, *J. Geophys. Res.*, *104*, 9135–9149, doi:10.1029/1999JD900076.

Mauersberger, K., and D. Krankowsky (2003), Vapor pressure above ice at temperatures below 170 K, *Geophys. Res. Lett.*, *30*(3), 1121, doi:10.1029/2002GL016183.

Murphy, D. M., and T. Koop (2005), Review of the vapor pressures of ice and supercooled water for atmospheric applications, *Q. J. R. Meteorol. Soc.*, *131*, 1539–1565, doi:10.1256/qj.04.94.

Petelina, S. V., D. A. Degenstein, E. J. Llewellyn, N. D. Lloyd, C. J. Mertens, M. G. Mlynczak, and J. M. Russell III (2005), Thermal conditions for PMC existence derived from Odin/OSIRIS and TIMED/SABER data, *Geophys. Res. Lett.*, *32*, L17813, doi:10.1029/2005GL023099.

Petelina, S. V., E. J. Llewellyn, and D. A. Degenstein (2007), Properties of polar mesospheric clouds measured by Odin/OSIRIS in the Northern Hemisphere in 2002–2005, *Can. J. Phys.*, *85*, 1143–1158, doi:10.1139/P07-092.

Rapp, M., and F.-J. Lübken (2004), Polar mesosphere summer echoes (PMSE): Review of observations and current understanding, *Atmos. Chem. Phys.*, *4*, 2601–2633.

Rapp, M., and G. E. Thomas (2006), Modeling the microphysics of mesospheric ice particles: Assessment of current capabilities and basic sensitivities, *J. Atmos. Sol. Terr. Phys.*, *68*, 715–744, doi:10.1016/j.jastp.2005.10.015.

Rusch, D. W. , et al. (2009), The cloud imaging and particle size experiment on the aeronomy of ice in the mesosphere mission: Cloud morphology for the northern 2007 season, *J. Atmos. Sol. Terr. Phys.*, *71*, 356–364, doi:10.1016/j.jastp.2008.11.005.

Russell, J. M., et al. (2009), Aeronomy of Ice in the Mesosphere (AIM): Overview and early science results, *J. Atmos. Sol. Terr. Phys.*, *71*, 289–299, doi:10.1016/j.jastp.2008.08.011.

Shettle, E. P., M. T. DeLand, G. E. Thomas, and J. J. Olivero (2009), Long term variations in the frequency of polar mesospheric clouds in the Northern Hemisphere from SBUV, *Geophys. Res. Lett.*, *36*, L02803, doi:10.1029/2008GL036048.

Sica, R. J., et al. (2008), Validation of the Atmospheric Chemistry Experiment (ACE) version 2.2 temperature using ground-based and space-borne measurements, *Atmos. Chem. Phys.*, *8*, 35–62.

Thomas, G. E. (2003), Are noctilucent clouds harbingers of global change in the middle atmosphere?, *Adv. Space Res.*, *32*, 1737–1746, doi:10.1016/S0273-1177(03)90470-4.

von Savigny, C., S. V. Petelina, B. Karlsson, E. J. Llewellyn, D. A. Degenstein, N. D. Lloyd, and J. P. Burrows (2005), Vertical variation of NLC particle sizes retrieved from Odin/OSIRIS limb scattering observations, *Geophys. Res. Lett.*, *32*, L07806, doi:10.1029/2004GL021982.

von Zahn, U., and U. Berger (2003), Persistent ice cloud in the midsummer upper mesosphere at high latitudes: Three-dimensional modeling and cloud interactions with ambient water vapor, *J. Geophys. Res.*, *108*(D8), 8451, doi:10.1029/2002JD002409.

P. F. Bernath, Department of Chemistry, University of York, Heslington YO10 5DD, UK.

C. D. Boone and R. Remorov, Department of Chemistry, University of Waterloo, Waterloo, ON N2L 3G1, Canada.

E. J. Llewellyn, Institute of Space and Atmospheric Science, University of Saskatchewan, Saskatoon, SK S7N 5E2, Canada.

S. V. Petelina, Department of Physics, La Trobe University, Melbourne, VIC 3086, Australia. (s.petelina@latrobe.edu.au)

A. Y. Zasetsky, Kurnakov Institute of General and Inorganic Chemistry, Russian Academy of Sciences, Moscow 117907, Russia.